# 10. High resolution transmission electron microscopy

High-resolution electron microscopy is a phase contrast microscopy of the atomic-level microstructure of materials. This technology can be used to image atomic strings in most crystal materials, called high-resolution imaging. The picture shows a high-resolution image of a face-centered cubic Si crystal along the [001] direction, in which the white bright spots are the projection of the Si atom strings.

High-resolution image of Si elemental crystal in [001] direction.

# Contents
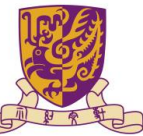
Transmission electron microscopes can be divided into:

Biological type: It is characterized by providing high contrast, the accelerating voltage is generally lower than 120 kV, and is mainly used in the biological and medical fields.

Analytical type: It is characterized by a large inclination angle of the sample stage and an accelerating voltage higher than 120 kV. It can realize in-situ analysis of microstructure, crystal structure and micro-area components and is used in fields such as materials science, physics, and chemistry.

High-resolution type: It is characterized by high resolution. The point resolution should be better than 0.2 nm. It is used to observe and analyze crystal defects, micro-domains, interfaces, and atomic arrangements on the surface. The accelerating voltage is 200 kV or above.

The above three types of electron microscopes mainly have different objective lens spherical aberration coefficients C_S due to differences in the structure of the objective lens pole piece. Reducing C_S is one of the ways to improve resolution.
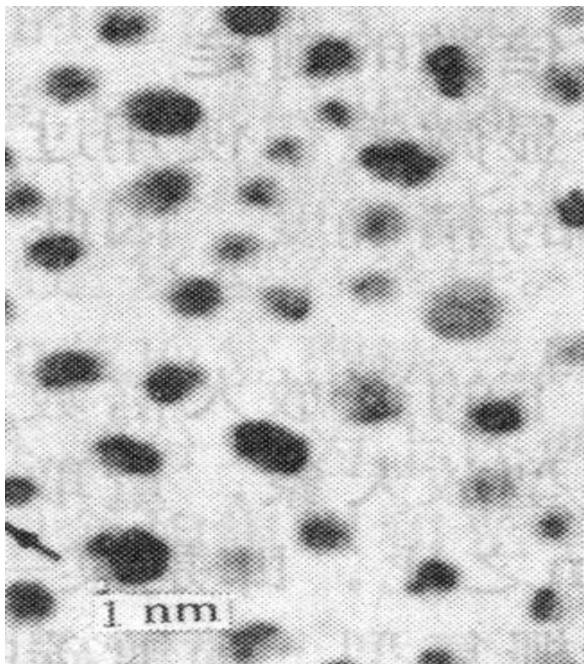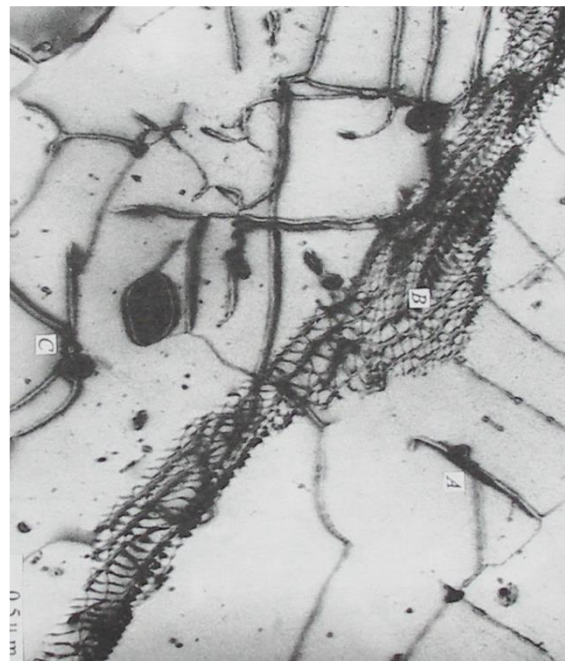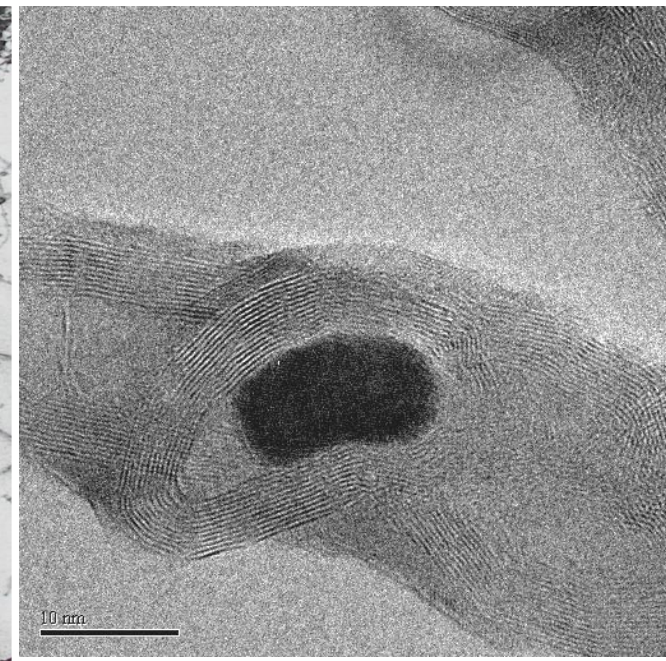
10.2 The principle of high-resolution electron microscopy
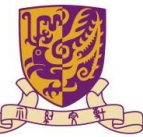

Thickness contrast
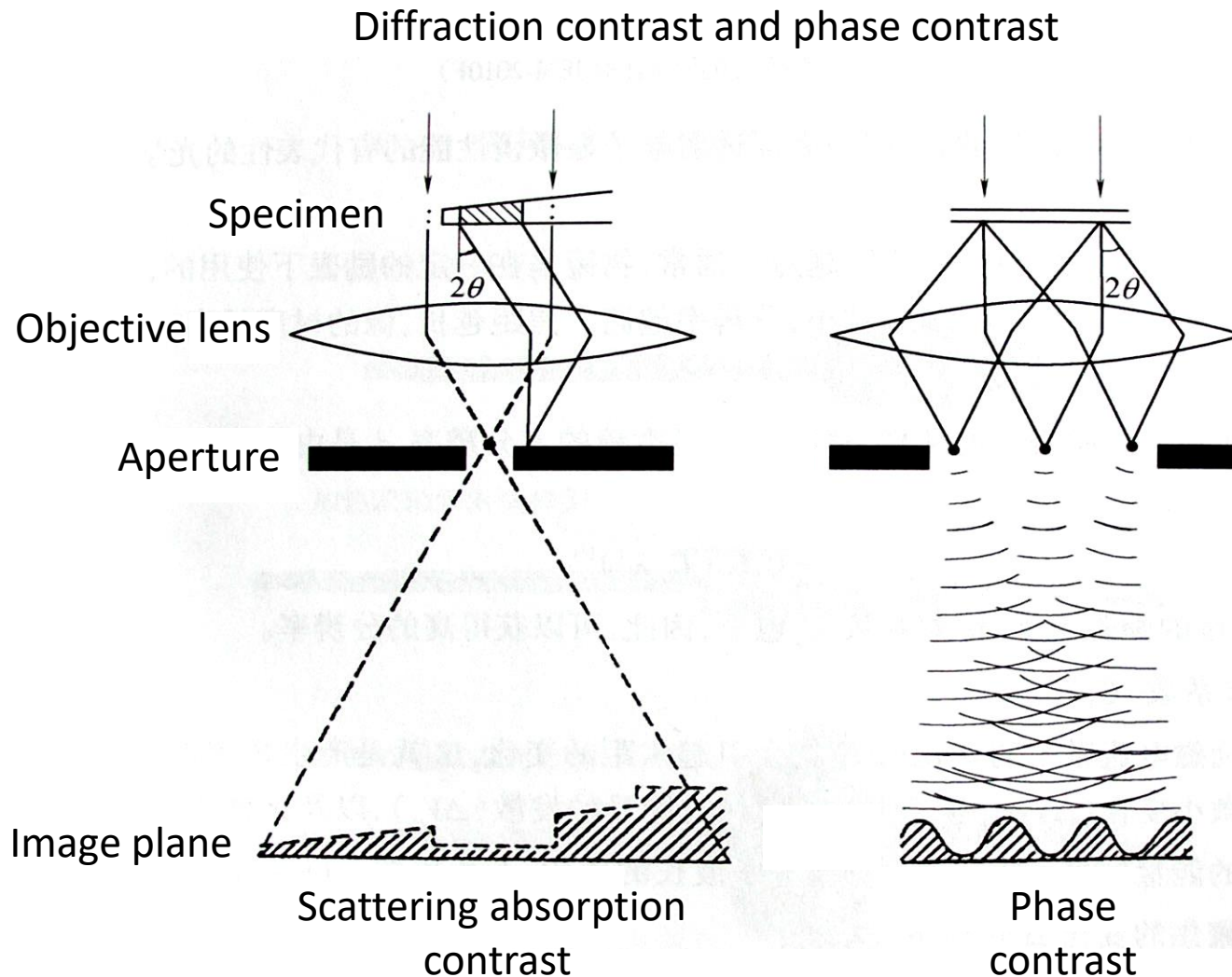
Diffraction contrast

Phase contrast

10.2 The principle of high-resolution electron microscopy

Diffraction contrast and phase contrast

Scattering absorption contrast

Phase contrast

10.2 The principle of high-resolution electron microscopy

1. Sample transmission function

Use the sample transmission function $q(x, y)$ to describe the scattering of the incident electron wave by the sample:

$$q(x, y) = A(x, y)\exp[i\varphi_t(x, y)]$$

In the formula, $A(x, y)$ is the amplitude, and $A(x, y) = 1$ is a single value; $\varphi_t(x, y)$ is the phase. When the sample is thin enough, there is:

$$\phi \approx \sigma \int V(x, y, z)dz = \sigma V_t(x, y)$$

In the formula, $\sigma = \pi/\lambda E$ is the interaction constant. The above equation shows that the total phase shift only depends on the crystal's potential function $V(x, y, z)$. Neglecting the minimal absorption effect, then:

$$q(x, y) = 1 + i\sigma V_t(\mathbf{x}, y)$$

This is the weak phase body approximation. The weak phase body approximation shows that for very thin samples, the transmission function is linearly related to the projection potential of the crystal, and only the two-dimensional projection potential $V_t(\mathbf{x}, y)$ of the crystal along the **z** direction is considered.

10.2 The principle of high-resolution electron microscopy

2. Contrast transfer function

The process by which electron waves pass through an objective lens and form a diffraction pattern on its back focal plane can be expressed by the contrast transfer function.

$$A(u) = R(u) \exp[i\chi(u)] \, B(u) \, C(u)$$

In the formula, u is the reciprocal vector; R is the objective lens aperture function; B and C are the attenuation envelope functions caused by the illumination beam divergence and chromatic aberration effect, respectively; χ is the phase difference.

$$\chi(u) = \pi \Delta f \, \lambda \, u^2 + 0.5\pi C_s \lambda^3 u^4$$

The objective lens spherical aberration coefficient C_s and the defocus amount Δf are the main factors affecting $\sin\chi$.
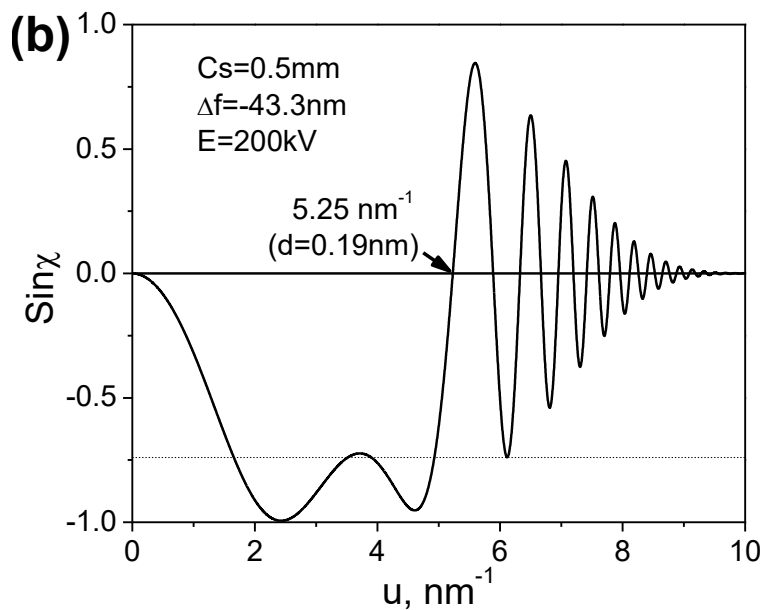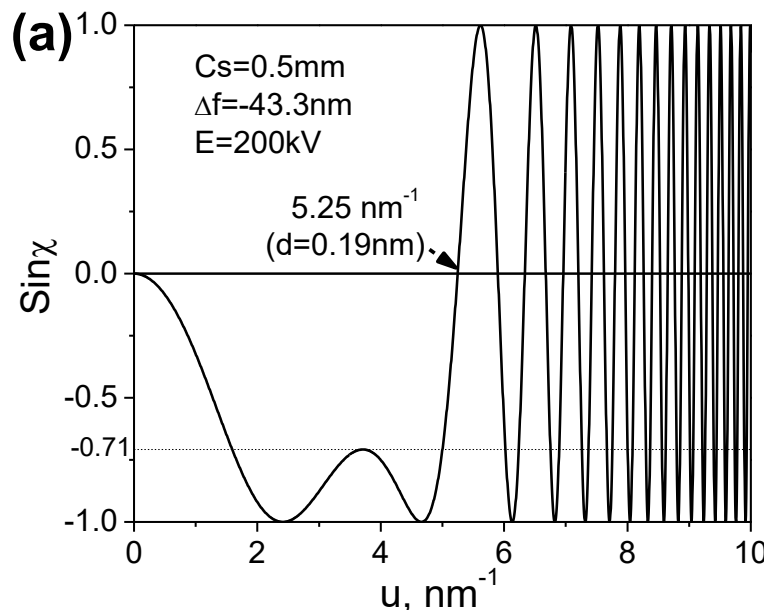
Under the optimal under-focus condition, the passband with an absolute value of 1 on the $\sin\chi$ curve is the widest. This is called the Scherzer under-focus condition. At this time, the point resolution of $\sin\chi$ is optimal.

10.2 The principle of high-resolution electron microscopy

2. Contrast transfer function

When the accelerating voltage of the JEM 2010 transmission electron microscope is 200 kV, Cs =0.5mm, $\Delta f = -43.3nm$ (optimal under-focus condition), its $\sin\chi$ function is shown in the figure, and the point resolution is 0.19 nm (the intersection of the curve and the horizontal axis) u = 5.25nm^{-1})
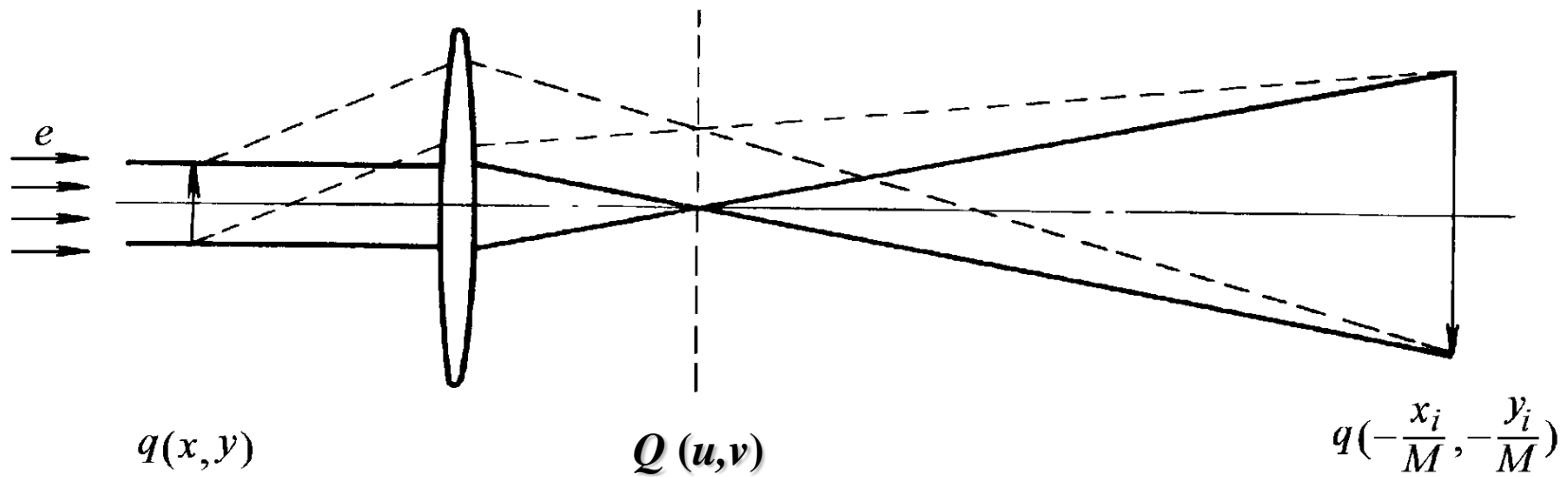

The $\sin\chi$ function (a) under optimal under-focus conditions of JEM 2010 transmission electron microscope and the comprehensive result after adding time and space envelope (b).

10.2 The principle of high-resolution electron microscopy

3. Phase contrast

After the electron wave passes through the crystal, it carries the structural information of the sample and is focused by the objective lens to form a diffraction pattern on the back focal plane of the objective lens. As a result of the mutual interference between the transmitted beam and the diffracted beam, a high-defined pattern is finally formed on the plane of the objective image. The formation process of high-resolution electron microscopy images is shown in the figure.

e

$q(x,y)$ $Q(u,v)$ $q(-\dfrac{x_i}{M},-\dfrac{y_i}{M})$
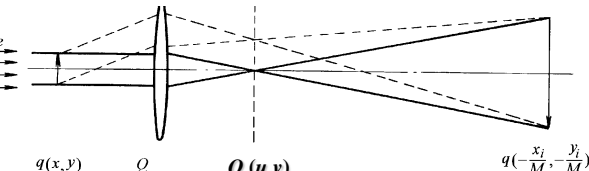
10.2 The principle of high-resolution electron microscopy

3. Phase contrast

The electron wave $q(x, y)$ passes through the objective lens and forms an electron diffraction pattern $Q(x, y)$ on the back focal plane.

$$Q(u, v) = F[q(x, y)]A(u, v)$$

In the formula, F is the Fourier transformation. $Q(u, v)$ undergoes another Fourier transformation, and an enlarged high-resolution image can be reconstructed on the image plane. Intensity distribution on the image plane is:

$$I(x, y) = 1 - 2\sigma V_t(x, y) * F[\sin\chi\,(u, v)\,RBC]$$

In the formula, $*$ represents the convolution operation. If the influence of RBC is not considered, the contrast of the image is

$$C(x, y) = I(x, y) - 1 = -2\sigma V_t(x, y)\,F\,[\sin\chi\,(u, v)]$$

When $\sin\chi = -1$,

$$C(x, y) = 2\sigma V_t(x, y)$$

Image contrast is proportional to the projection potential of the crystal and can reflect the true structure of the sample.
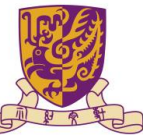
10.2 The principle of high-resolution electron microscopy

4. The influence of under-focus and sample thickness on image contrast

Only high-resolution images taken under weak phase body approximation and optimal under-focus conditions can correctly reflect the crystal structure. However, the requirements of weak phase body approximation are difficult to meet.
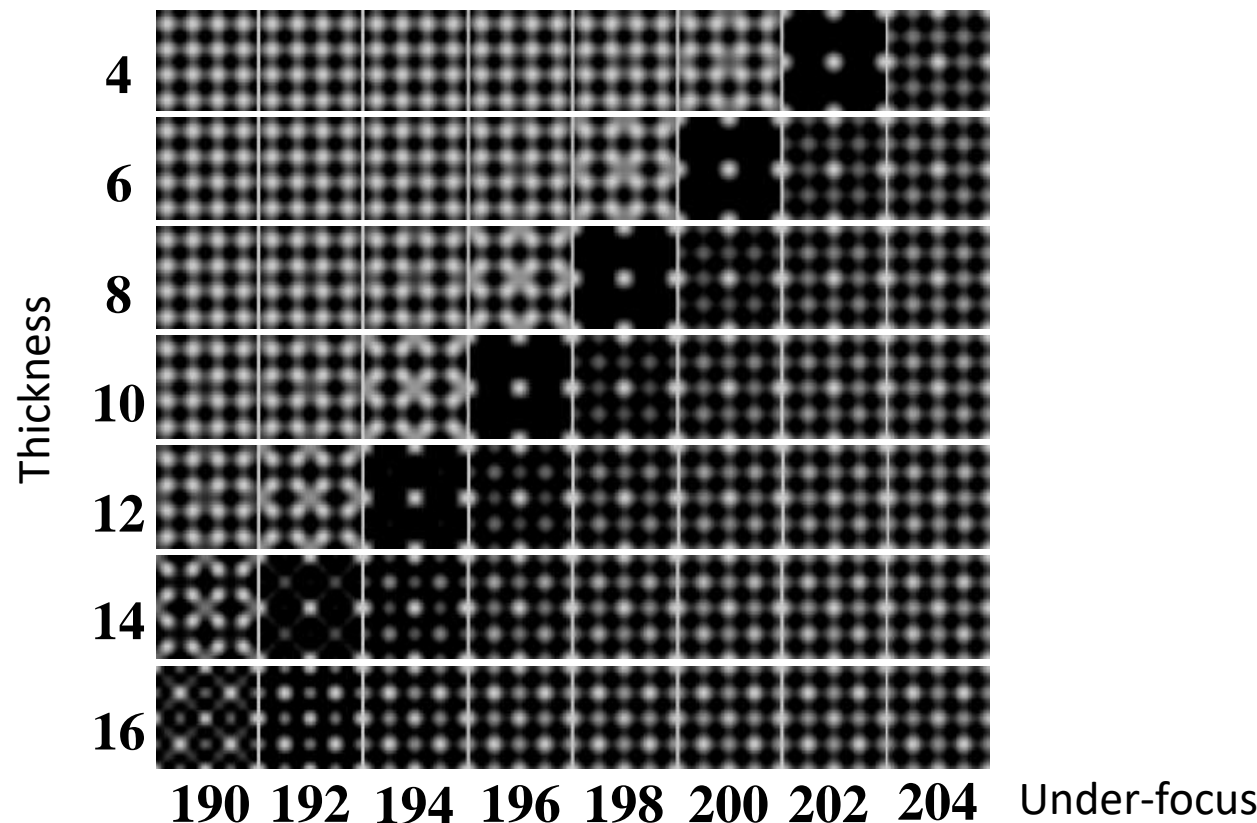
When the weak phase body approximation conditions are not met, although a clear high-resolution image can still be obtained, there is no one-to-one correspondence between image contrast and crystal structure projection. As the defocus amount and specimen thickness change, image contrast will appear. Degree reversal; image point distribution patterns will also change.

10.2 The principle of high-resolution electron microscopy

4. The influence of under-focus and sample thickness on image contrast

It can be seen from the figure that as the amount of under-focus and thickness change, the distribution pattern of image points changes significantly. Only (under-focus, thickness) is (-192, 14), (-194, 12), (-196, 10), (-198, 8), (-200, 6), (-202, 4). Under other conditions, the bright spots represent the projection position of **Y** atoms in the $Y_{0.25}Zr_{0.75}O_{2-x}$ phase.
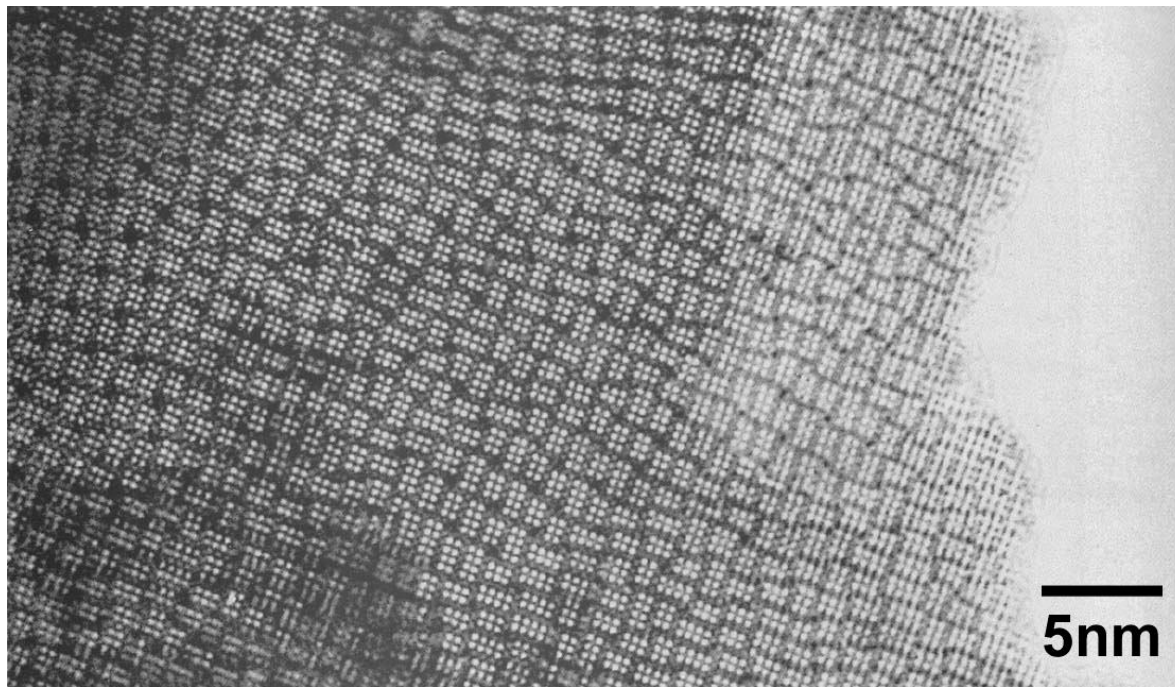
Thickness (4, 6, 8, 10, 12, 14, 16) vs Under-focus (190, 192, 194, 196, 198, 200, 202, 204)

10.2 The principle of high-resolution electron microscopy

4. The influence of under-focus and sample thickness on image contrast

The figure shows high-resolution photos of Nb_2O_5 single crystals in different sample thickness areas under the same under-focus. It can be seen that from the edge of the sample to the inside, the regional changes in image contrast are caused by uneven thickness.


5nm
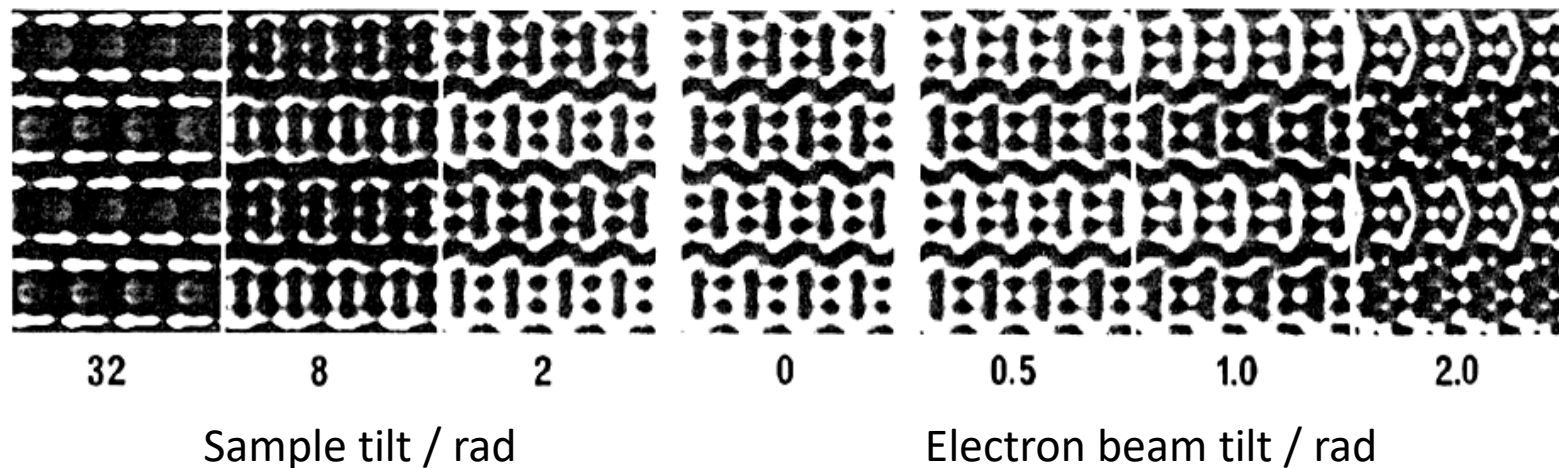
High-resolution image contrast changes with sample thickness (Nb_2O_5).

10.2 The principle of high-resolution electron microscopy

5. Effects of electron beam tilt and sample tilt on image contrast

Both the electron beam tilt and the sample tilt will affect the high-resolution image contrast. A slight tilt of the electron beam will introduce an asymmetric phase shift in the diffraction beam. Figure shows the high-resolution simulation image of the $Ti_2Nb_{10}O_{29}$ sample when the thickness is 7.6 nm. The figure clearly shows that even a slight tilt of the electron beam or sample will significantly impact the high-resolution image's contrast.

| 32 | 8 | 2 | 0 | 0.5 | 1.0 | 2.0 |

Sample tilt / rad Electron beam tilt / rad

Effect of electron beam and sample tilt on the contrast of $Ti_2Nb_{10}O_{29}$ simulated high-resolution image.

10.2 The principle of high-resolution electron microscopy

6. Computer simulation of high-resolution images

- Applications
1) Interpret the high-resolution images obtained from the experiment.
2) Confirm the unknown crystal structure by matching simulated images and experimental images.
3) Obtain certain phenomena that cannot be observed in experiments.

- Simulation method
Mainly composed of two methods: Bloch wave and multi-layer method.

- The main steps
1) Establish a structural model of crystals or defects.
2) Propagation of the incident electron beam through the crystal layer.
3) Transmission of scattered waves by the electron microscope optical system.
4) Quantitative comparison of simulated images and experimental images.

6. Computer simulation of high-resolution images

The Bloch wave method directly solves the time-independent Schrödinger equation and is mainly used for simulation calculations of small complete unit cells; the multi-layer method is based on the physical optics approximation, and its process can be described by the Fresnel approximation of the Rayleigh-Sommerfeld diffraction formula (Figure 1). The slice method series projection and propagation are shown in Figure 2.
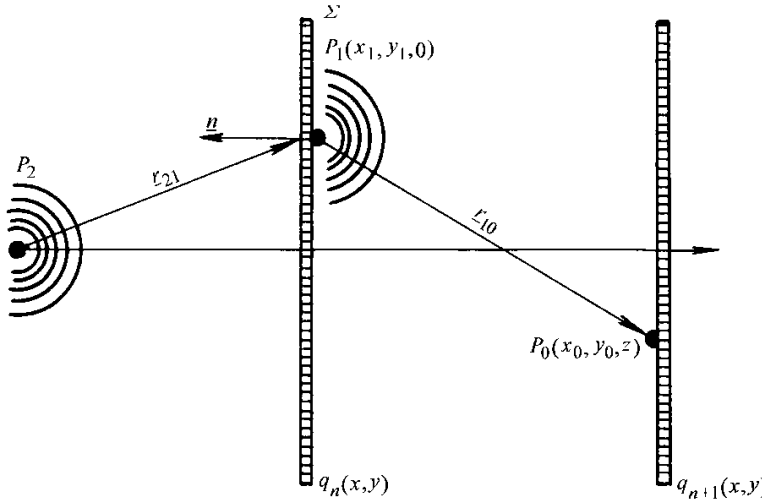

Figure 1: The diffraction situation when an incident wave passes through an object with a composite transfer coefficient of $qn(x, y)$.
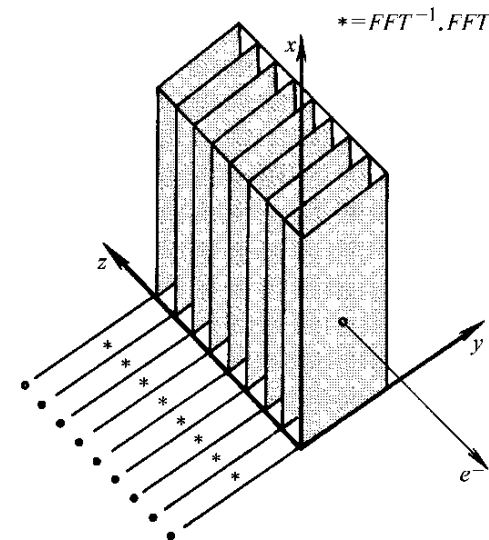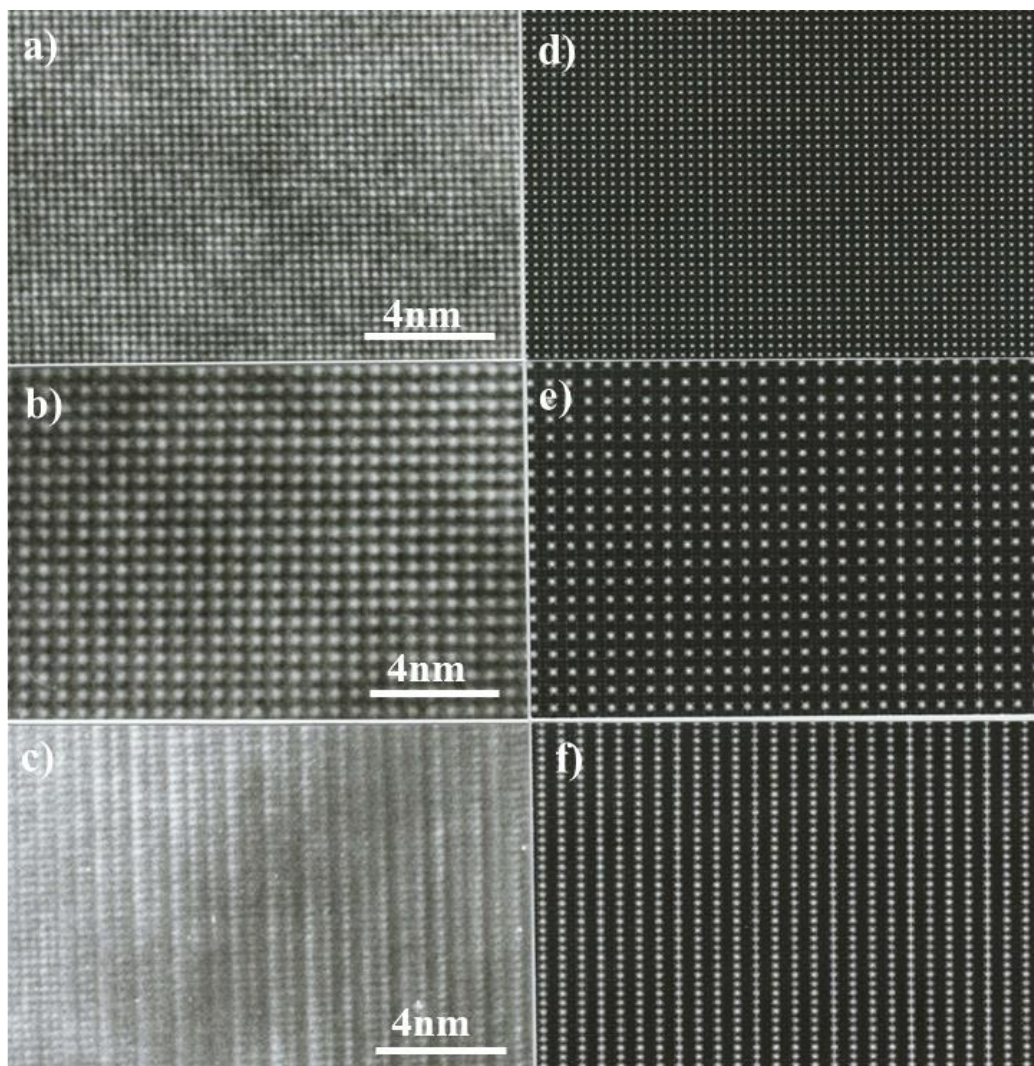

Figure 2: Schematic diagram of multi-layer method series projection and propagation.

10.2 The principle of high-resolution electron microscopy

6. Computer simulation of high-resolution images

Experimental images a), b), c) and simulated high-resolution images d), e), f) of $c\text{-}ZrO_2$, $Y_{0.25}Zr_{0.75}O_{2-x}$ and $Y_{0.5}Zr_{0.5}O_2$ phases.

10.3 Applications of high-resolution transmission electron microscopy in materials science

The microstructure and defect structure of materials significantly impact materials' physical, chemical, and mechanical properties. High-resolution electron microscopy can be used to study the microstructure and defects of materials at the atomic scale. Its applications mainly include:

1) Study of crystal defect structure
2) Research on interface structure
3) Research on surface structure
4) Research on various material structure

Some typical high-resolution images are given below to illustrate the application of high-resolution transmission electron microscopy in the analysis and research of materials' atomic-scale microstructure, surface and interface, and nano-powder structure.
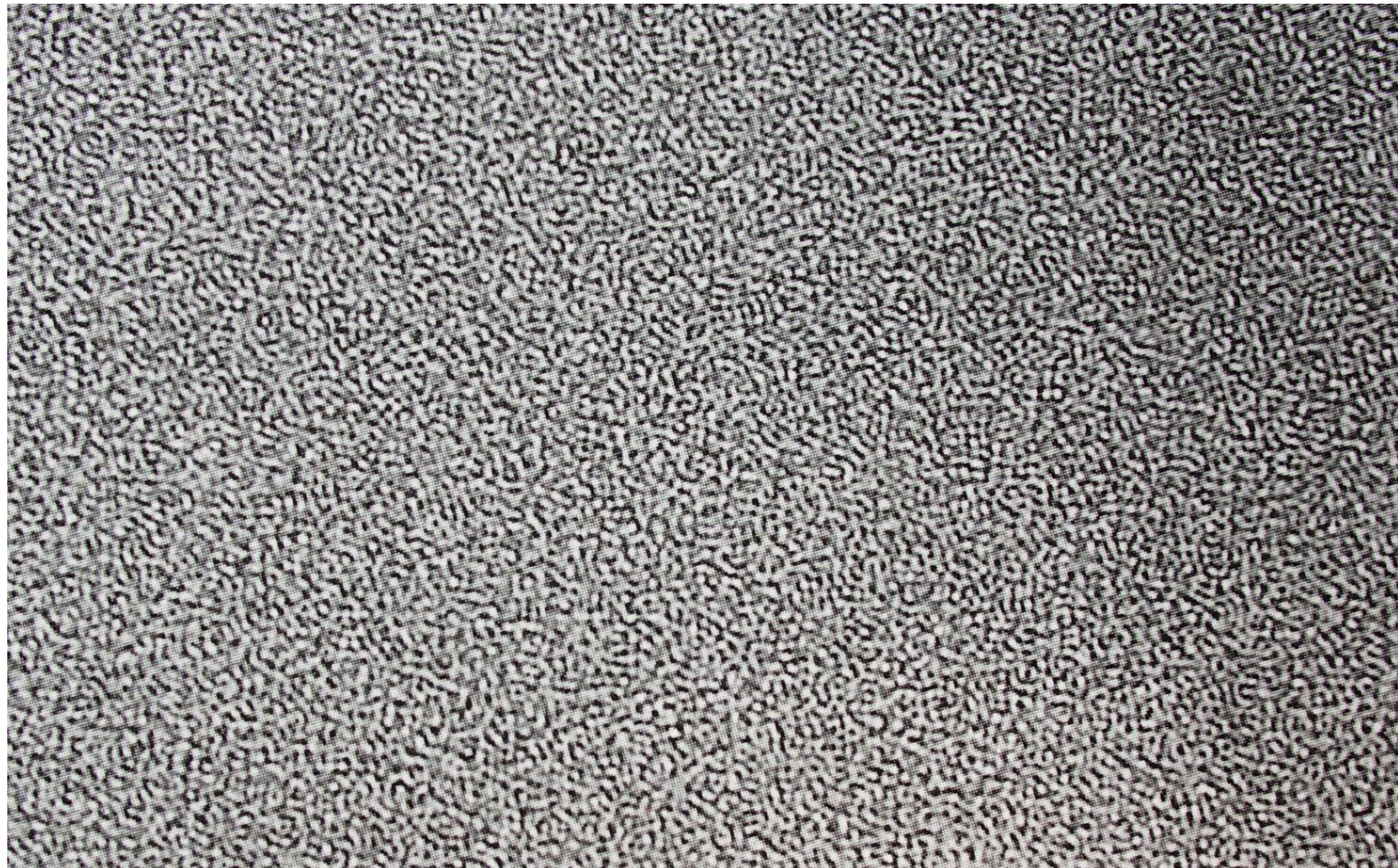
10.3 Applications of high-resolution transmission electron microscopy in materials science

7. Application examples—amorphous high-resolution images

10.3 Applications of high-resolution transmission electron microscopy in materials science

7. Application examples

The picture shows a high-resolution structural image along the *c*-axis direction of the α and β-Si_3N_4 phases. The dark spots in the photo correspond to the positions of the atoms.
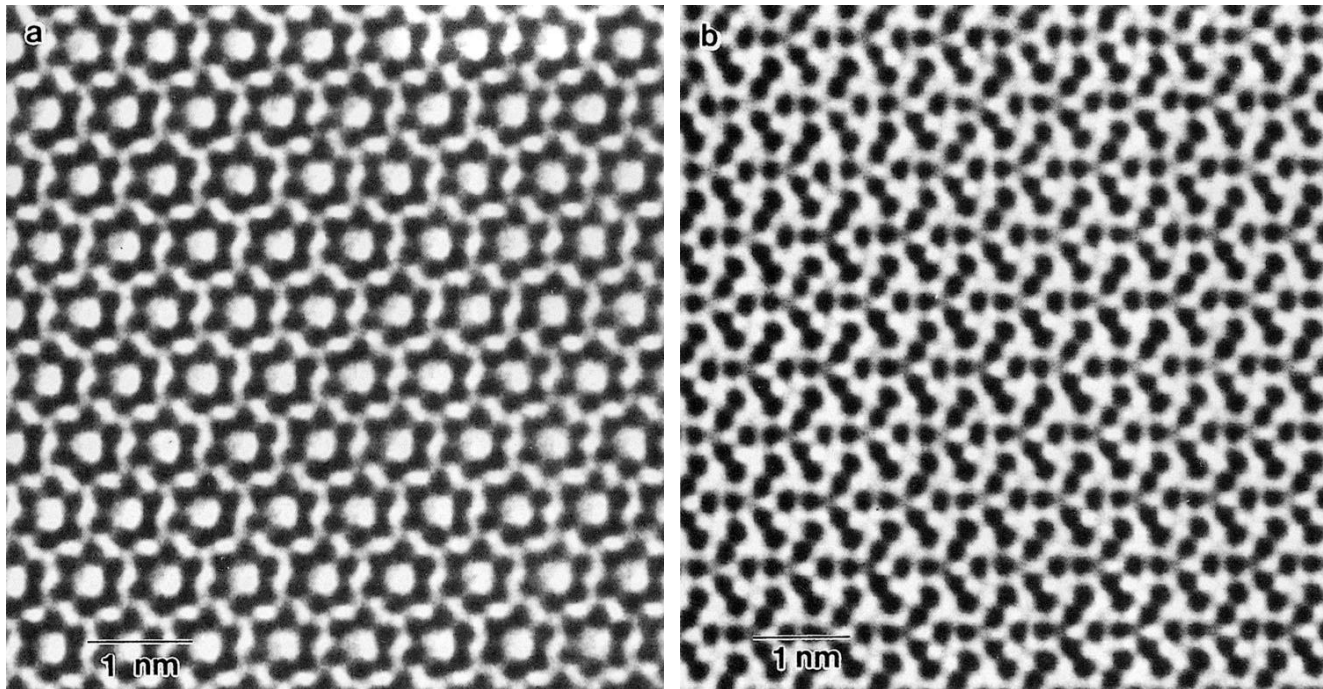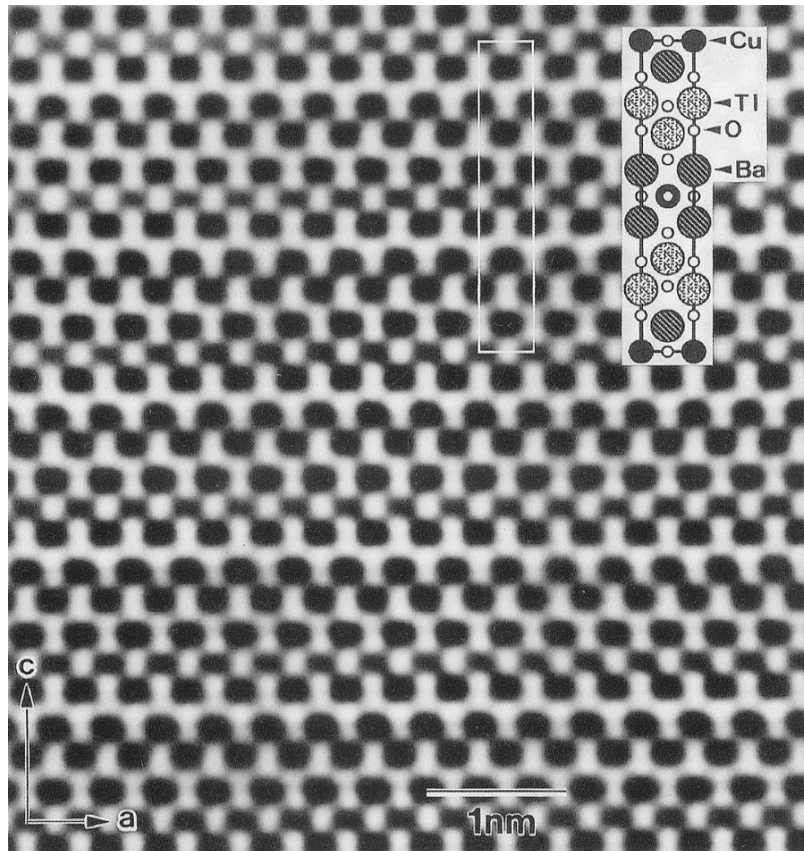

Figure: High-resolution structural images of silicon nitride a) α -Si_3N_4 and b) β-Si_3N_4

10.3 Applications of high-resolution transmission electron microscopy in materials science

7. Application examples

As shown in Figure, the large dark spots correspond to the positions of Tl and Ba heavy atoms, and the small dark spots correspond to the positions of Cu atoms.
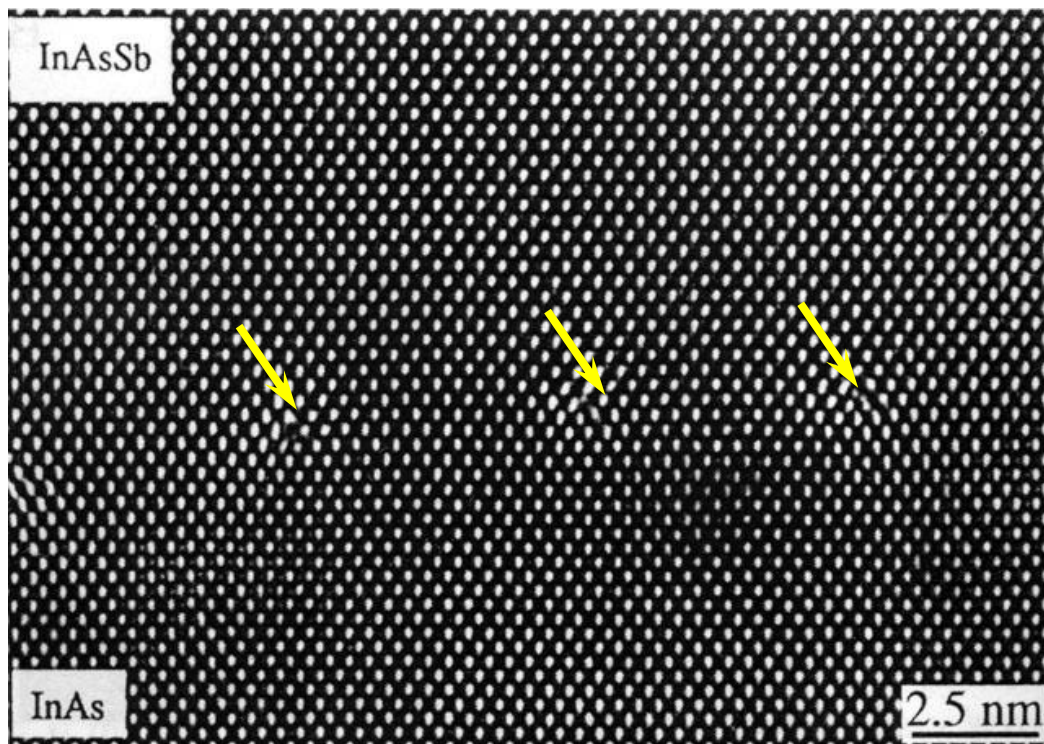

High-resolution structural image of $Tl_2Ba_2CuO_6$ superconducting oxide.

10.3 Applications of high-resolution transmission electron microscopy in materials science

7. Application examples

The figure shows that edge dislocations can be clearly observed at the interface between **InAs** and **InAsSb**. The arrow shows the location in the figure.
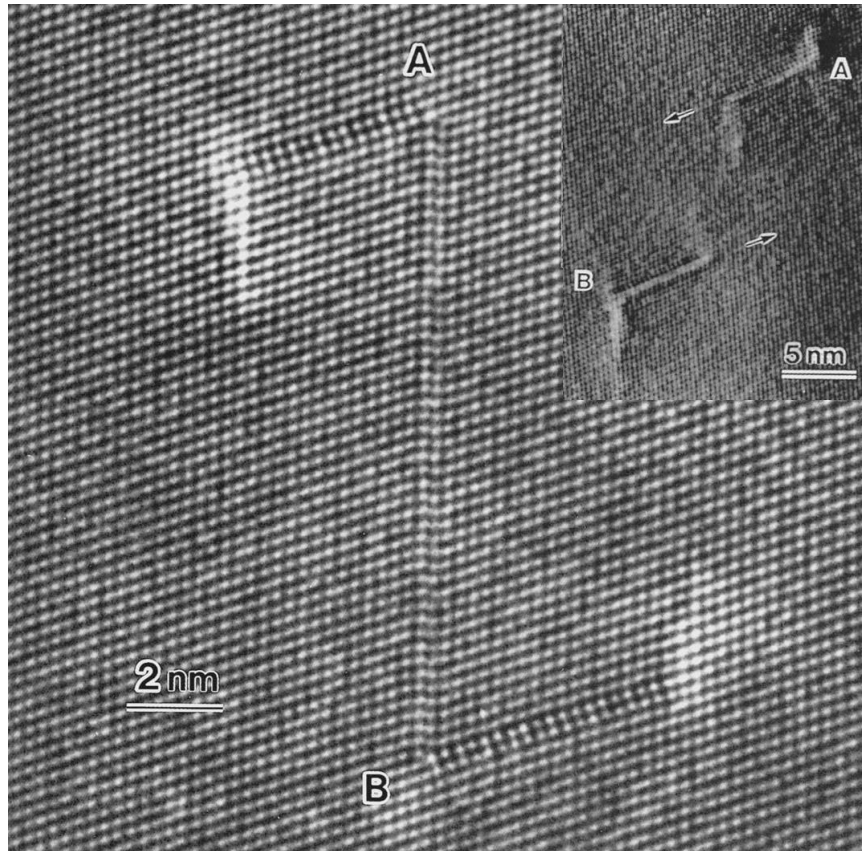

High-resolution image of the interface between semiconductor materials **InAs** and **InAsSb**.
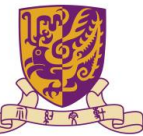
10.3 Applications of high-resolution transmission electron microscopy in materials science

7. Application examples

As shown in the figure, there is a ductile dislocation at A and B, and a stacking fault is sandwiched between AB, which is called a Z-shaped stacking fault dipole.
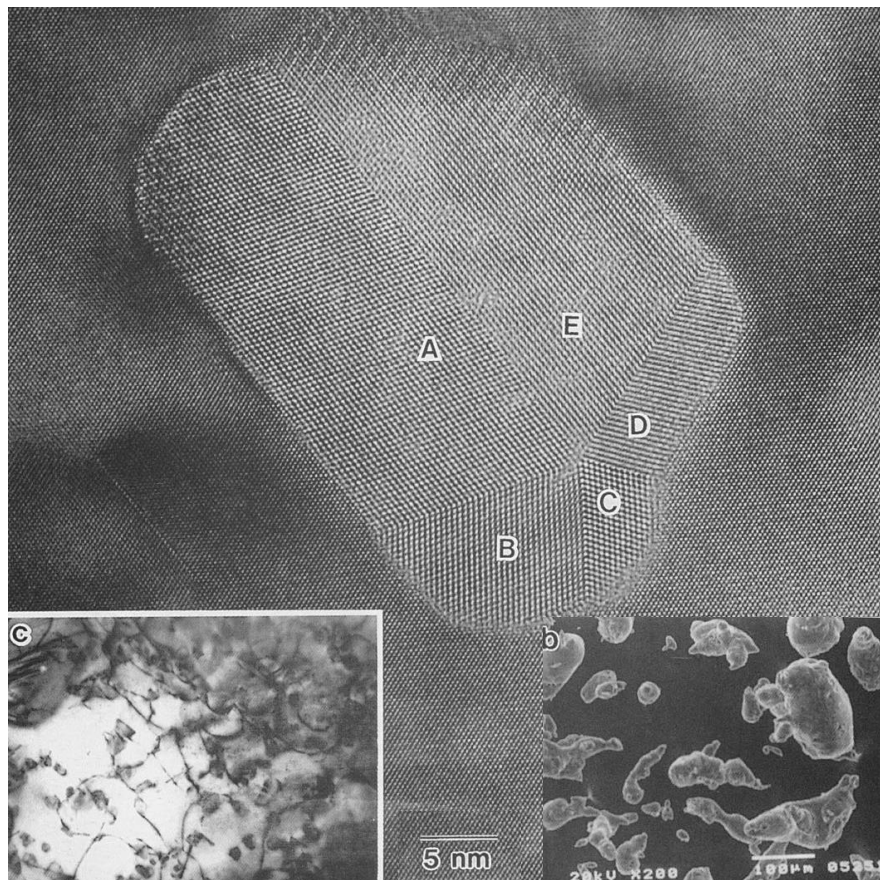

High-resolution lattice image of stacking fault dipoles in Si single-crystal.
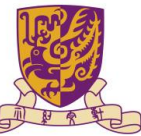
10.3 Applications of high-resolution transmission electron microscopy in materials science

7. Application examples

As shown in the figure, there are five twins A, B, C, D, and E in the Si particles, and the [110] direction of Al is parallel to the [110] direction of Si.
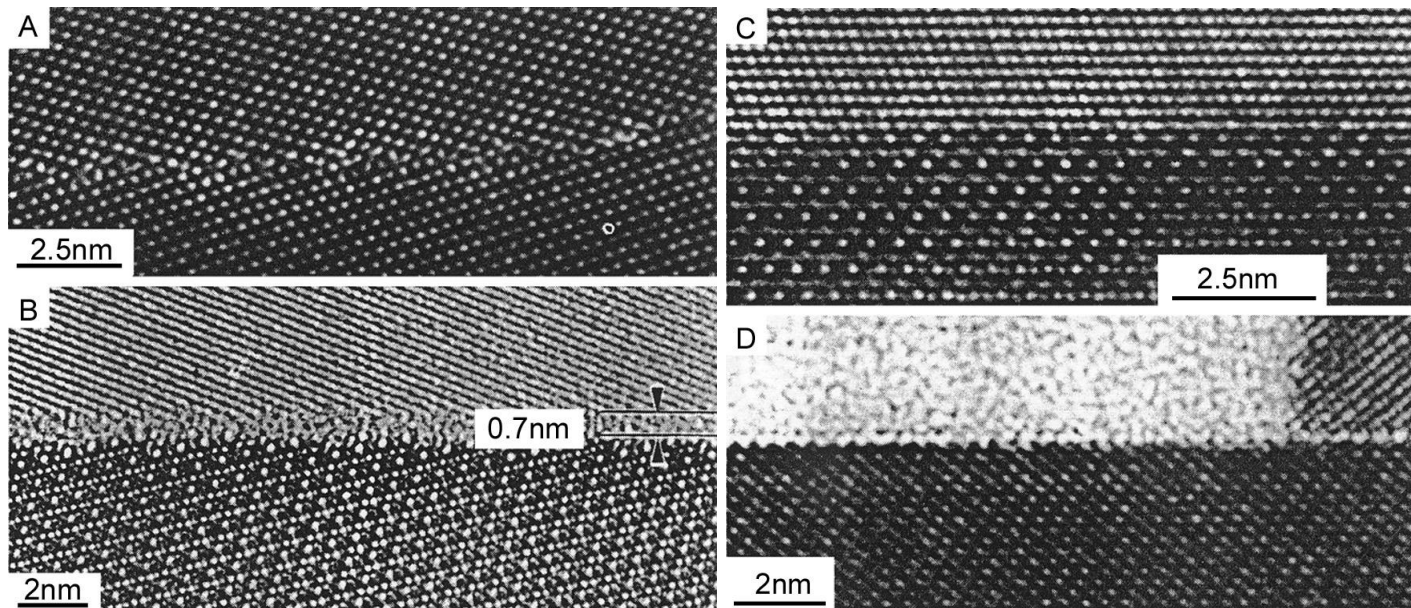

High-resolution image a), SEM image b) and TEM bright field image c) of Al-Si alloy powder.

10.3 Applications of high-resolution transmission electron microscopy in materials science

7. Application examples

It can be seen from the figure that there is an amorphous layer on the Si_3N_4 grain boundary, the phase boundary between $NiAl_2O_4$ and NiO is a stable interface, and the Fe_2O_3 surface is its (0001) plane.
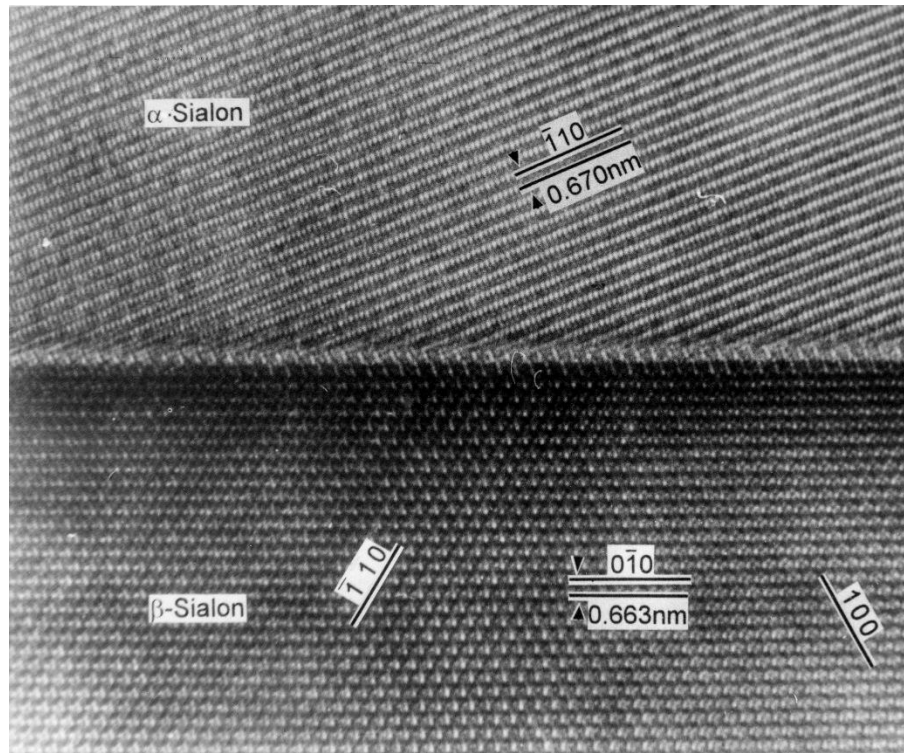

High-resolution images of several planar interfaces a) The grain boundary of Ge b) The grain boundary of Si_3N_4 c) The phase boundary between NiO and $NiAl_2O_4$ d) The surface profile of Fe_2O_3.

26

10.3 Applications of high-resolution transmission electron microscopy in materials science

7. Application examples

It can be seen from the figure that the lattice of the ($\bar{1}00$) plane of the α phase and the (100) plane of β the phase is directly combined, there is no amorphous layer at the interface, and the phase interface is a stable interface parallel to $(010)_\beta$.
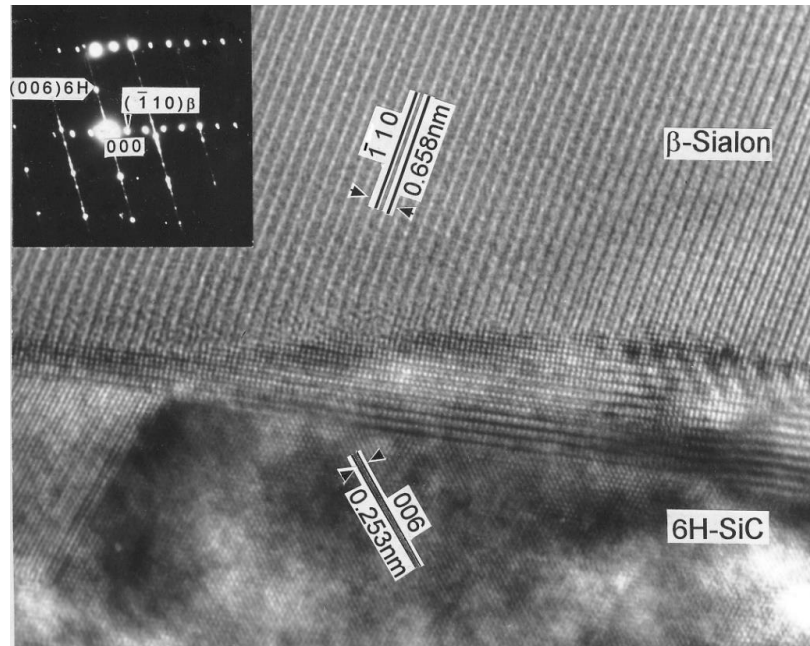
High-resolution image of α / β **Sialon** flat phase interface.

10.3 Applications of high-resolution transmission electron microscopy in materials science

7. Application examples

The figure shows a high-resolution image of the interface between **SiC** particles and Sialon ceramics. The **β-Sialon** phase ($\bar{1}$10) plane is directly combined with the (006) crystal plane of **6H-SiC** without an amorphous layer.
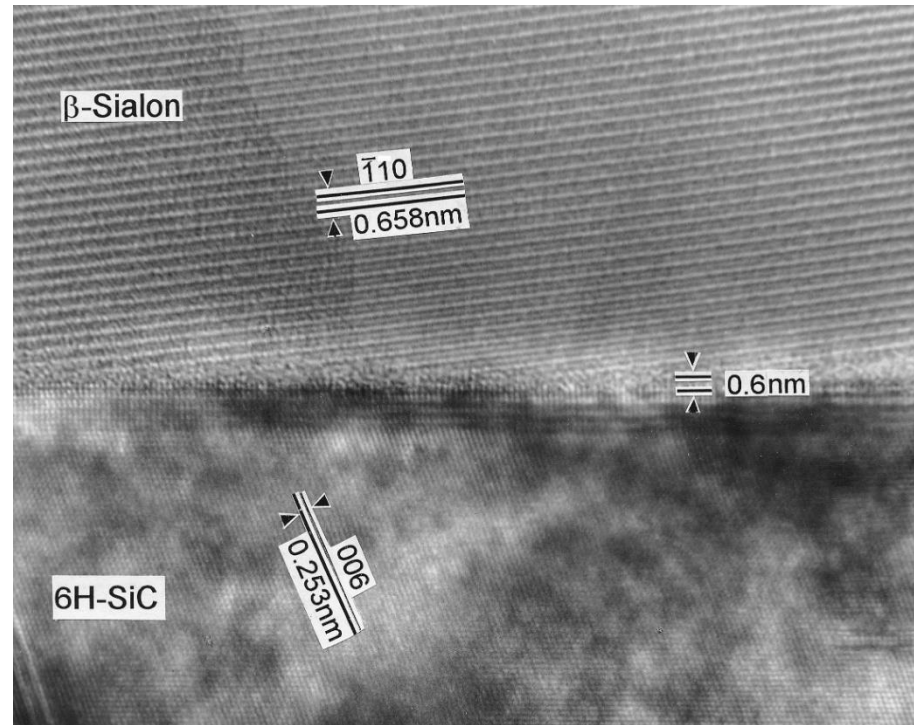
High-resolution image of the direct bonding interface between
SiC particles and Sialon ceramics.
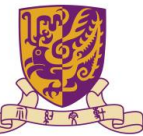
10.3 Applications of high-resolution transmission electron microscopy in materials science

7. Application examples

The figure shows a high-resolution image of the interface between SiC particles and Sialon ceramics. It can be seen that there is an amorphous layer with a thickness of about 0.6nm at the phase interface.
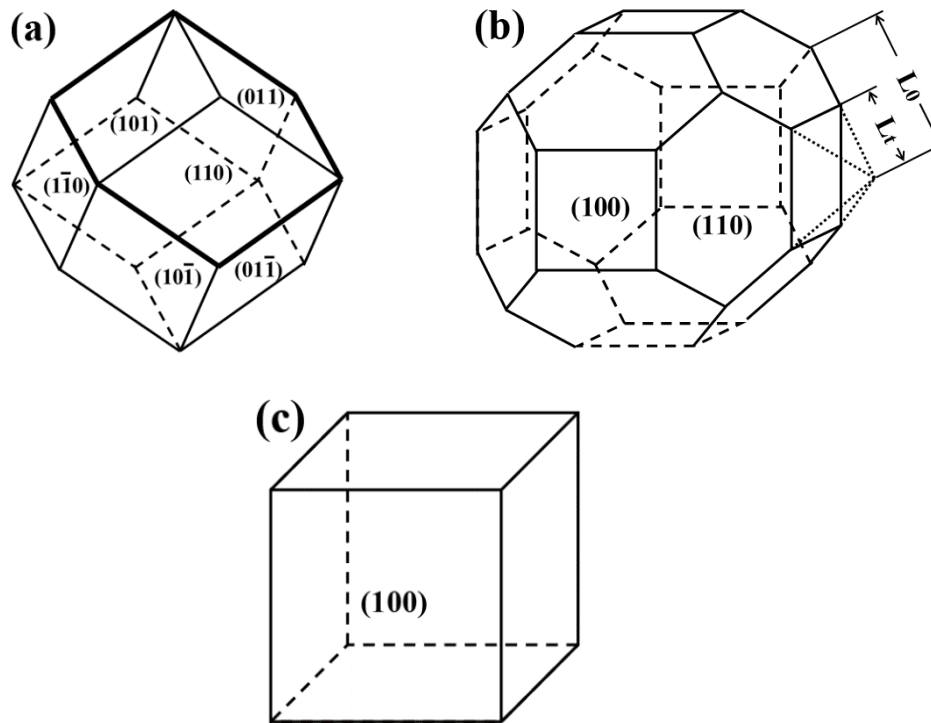

High-resolution image of the interface between SiC particles and Sialon ceramics.

10.4 Examples of high-resolution transmission electron microscopy

1. Epitaxial passivation oxide film on the surface of metal nanoparticles

Schematic diagram of the evolution process from rhombic dodecahedron to cubic crystal: (a) rhombic dodecahedron, (b) truncated rhombic dodecahedron (truncation degree R=Lt/L0), (c) cube

10.4 Examples of high-resolution transmission electron microscopy
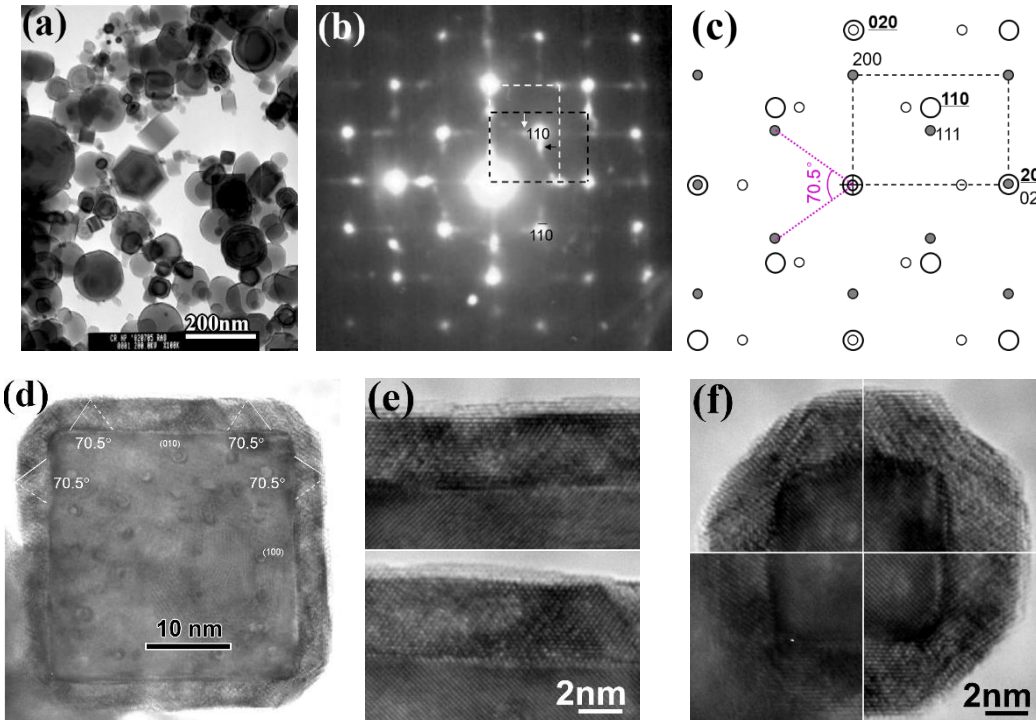
1. Epitaxial passivation oxide film on the surface of metal nanoparticles

It is known that the surface oxide of bulk metal chromium is Cr_2O_3, which is similar to α-Al_2O_3 with a rhombic structure. The results of this study show that the crystallographic results of the epitaxial passivation oxide film of Cr nanoparticles are related to the crystal plane on which they grow. The truncated Cr nanoparticle is an 18-hedron composed of 6 {100} faces and 12 {110} faces. Although α-Cr_2O_3 with a rhombohedral structure was generated on the {110} crystal plane, an unreported face-centered cubic structure of Cr_2O_3 was found on the {100} plane, and its lattice constant was determined to be 0.407 by accurate electron diffraction data. nm. Under normal temperature and pressure, an epitaxial dense inert oxide film is formed on the surface of pure Cr nanoparticles, which is only 3-4nm thick. This dense oxide film allows pure metal nanoparticles to be stored in water for several years without deterioration. Studies have found that the surface of pure Fe nanoparticles also has similar oxides.

10.4 Examples of high-resolution transmission electron microscopy

1. Epitaxial passivation oxide film on the surface of metal nanoparticles
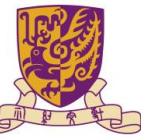
TEM study of Cr nanoparticles (Particle 1): (a) TEM bright field morphology image, (b) diffraction spectrum of a single 100% intercepted cubic particle, (c) decomposition diagram of complex diffraction spectrum, (d) High-resolution image of the particle, (e) high-resolution image of the oxide film on the {100} surface, (f) high-resolution image of the oxide film at the four vertex corners.

10.4 Examples of high-resolution transmission electron microscopy
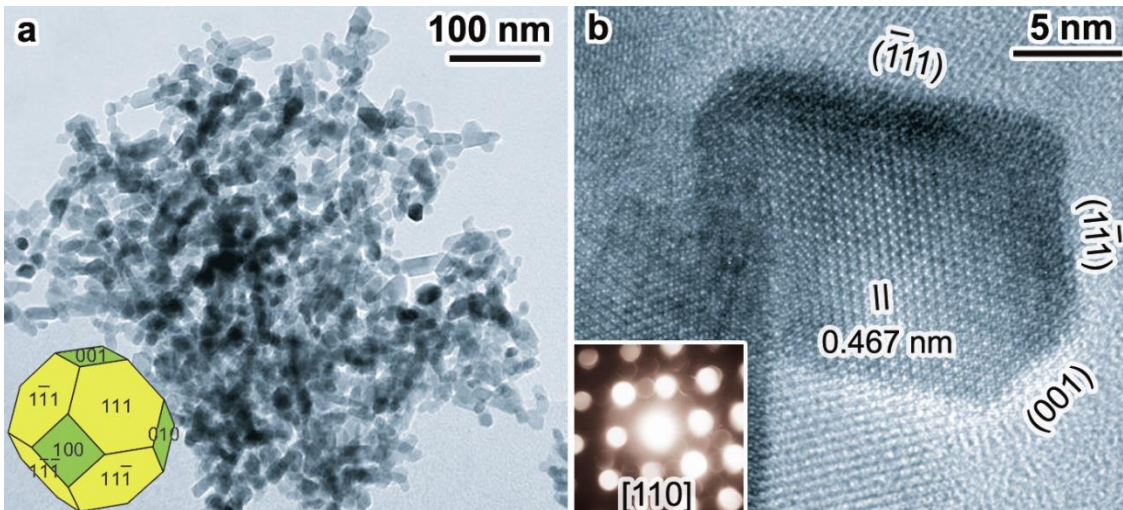
2. Morphology effect of cobalt tetroxide catalytic materials Co_3O_4

Co_3O_4 nanorods prepared through morphology control preferentially expose the {110} crystal face (accounting for more than 40%) and contain more Co^{3+} active centers, so they have incredibly high CO low-temperature oxidation activity and water resistance. 100% CO conversion rate can be obtained, and its reaction rate is more than 10 times that of Co_3O_4 nanoparticles, which is the best result of low-temperature CO oxidation reported. This research proves the morphology effect in nano-catalysis at the molecular level. It breaks through the problem of low-temperature CO catalytic oxidation of metal oxides in the presence of water vapor.
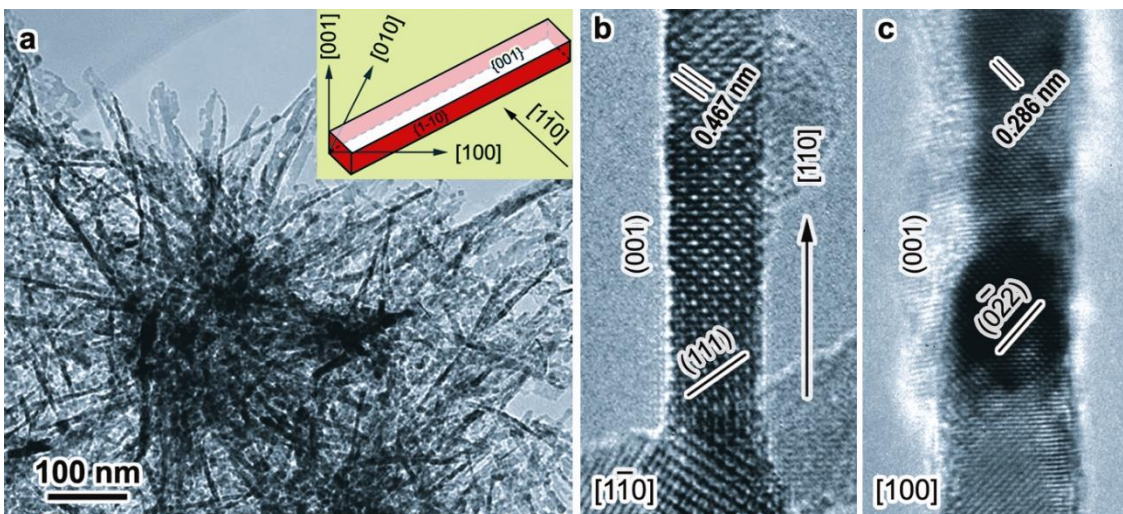
10.4 Examples of high-resolution transmission electron microscopy

2. Morphology effect of cobalt tetroxide catalytic materials Co_3O_4

Morphology and surface exposed crystal facets of Co_3O_4 nanoparticles.

Morphology and surface exposed crystal facets of Co_3O_4 nanorods.

10.4 Examples of high-resolution transmission electron microscopy

2. Morphology effect of cobalt tetroxide catalytic materials Co_3O_4

The number of Co3+ ions in different crystal planes and adjacent atomic layers of Co3O4 crystal

Plane	Unit area	Co^{3+} number in crystal plane	adjacent upper and lower atomic layers Co^{3+} number
{110}	$\sqrt{2}\,a^2$	4	$3 + 3 = 6$
{100}	a^2	0	$4 + 4 = 8$
{111}	$\sqrt{3}\,a^2$	0	$3 + 1 = 4$
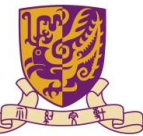
10.4 Examples of high-resolution transmission electron microscopy

## 3. Surface structure of ultra-large unit cell materials
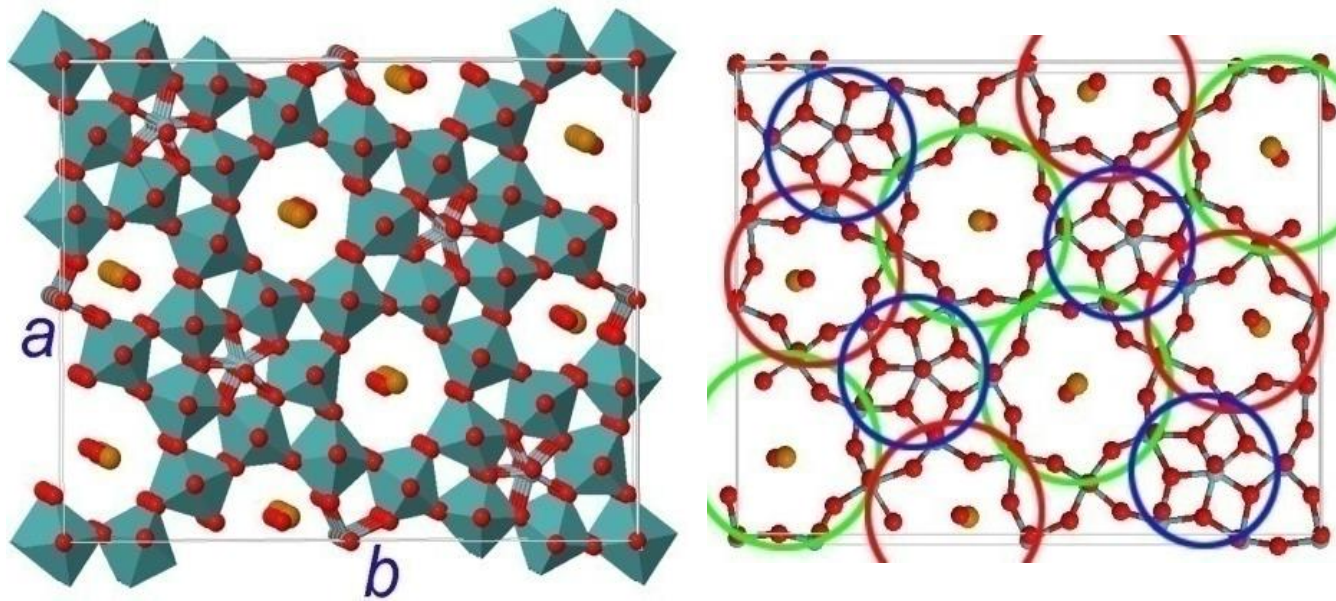
Viewing the surface structure of materials from real space has always been a challenge, especially for complex oxides. The key catalyst for the oxidation of propane to acrylic acid and acrylonitrile - the super large unit cell M1 phase (the unit cell contains 5 elements including Mo, V, Te, Nb, O, etc., totaling about 180 atoms) has a very complex structure, with regular five circles inside Rings, six-ring and seven-ring channels, as well as the complex occupancy of oxygen atoms. The crystal structure parameters of the M1 phase are as follows: Orthorhombic crystal system, space group code is Pba2 (32), lattice parameters a =2.11, b=2.67, c= 0.40 nm, $\alpha=\beta=\gamma=90\,^{\circ}$.

The study found that the surface layer of the M1 phase terminates in incomplete unit cells and accurately analyzed its surface structure, providing key evidence for understanding the catalytic mechanism.

10.4 Examples of high-resolution transmission electron microscopy

3. Surface structure of ultra-large unit cell materials

Crystal model of the complex unit cell M1 phase (full version on the left, simplified version on the right) $(\mathbf{Mo,V,Nb})\mathbf{O_6}$ octahedron constructs a non-close-packed complex network with a thickness of 0.4 nm composed of a pentagonal bipyramidal "O×O cluster".

## 10.4 Examples of high-resolution transmission electron microscopy

4. Atomic displacement and ferroelectric effect of ferroelectric materials
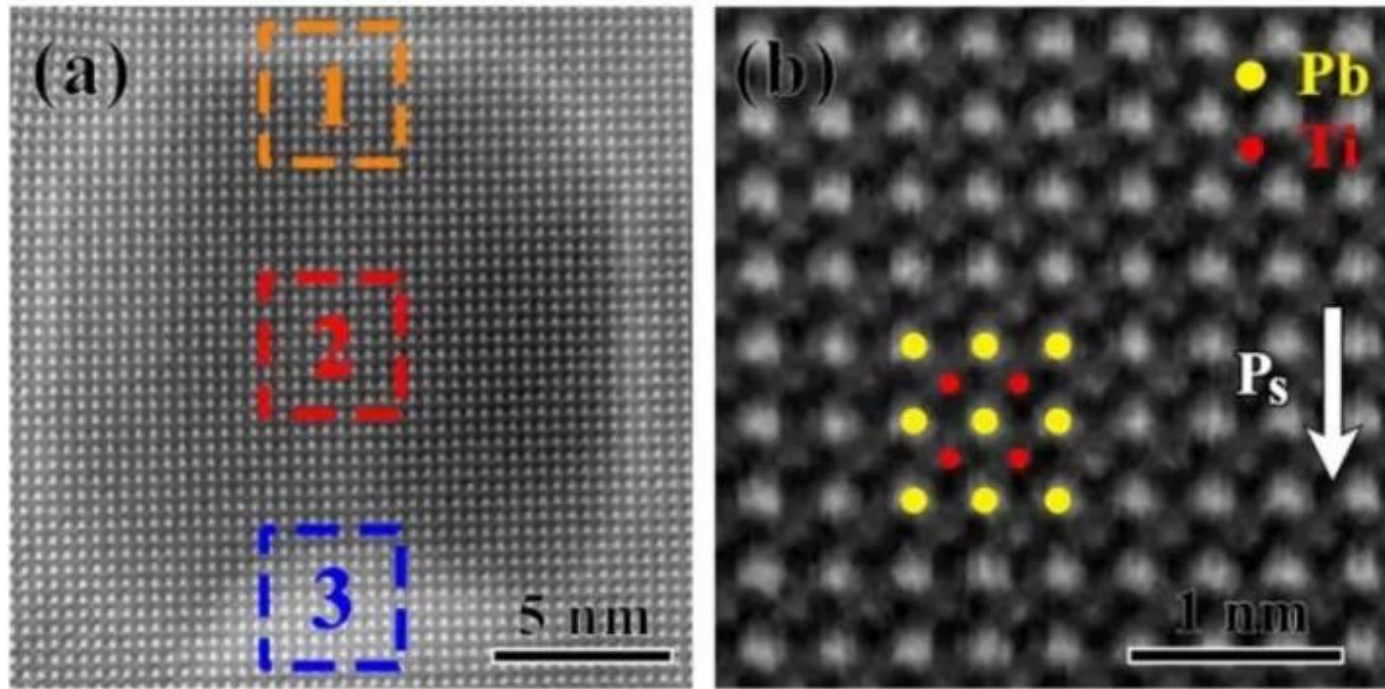
In physics and materials research, solutions to many problems have been put on hold due to factors such as sample quality, size, and detection limits. However, these problems can be solved through electron microscopy methods. Advanced electron microscopy methods such as spherical aberration correction developed in recent years have made it possible to measure and characterize many physical quantities and their coupling relationships at the nanometer and even atomic scales. They also provide a basis for nanoscale structural design to achieve performance control.

In strongly correlated electronic systems such as transition metal oxides, electrons exhibit charge and complex properties such as spin and orbit. The mutual coupling gave birth to products such as high-temperature superconductivity, giant magnetoresistance, multiferroicity, etc. Many features with important application prospects. However, the understanding of the coupling relationship between charge, orbit, and spin and the coupling and interaction between order and crystal lattice is still insufficient, which restricts the exploration of effective regulation of the properties of such functional materials.

10.4 Examples of high-resolution transmission electron microscopy

4. Atomic displacement and ferroelectric effect of ferroelectric materials

High-resolution high-angle annular dark field scanning transmission (HAADF-STEM) image (a) and magnified image of area 2 (b) of the area around a single mesopore of mesoporous lead titanate (PTO) fiber. The positions of Pb and Ti atoms are, respectively. It is marked schematically in the picture with yellow and red dots.